

Oriental Distribution Function of Aligned Elongated Molecules and Particulates Determined from Their Scattering Signature

Guan-Rong Huang,^{*,†} Yangyang Wang,[‡] Changwoo Do,[†] Yuya Shinohara,[§] Takeshi Egami,^{§,||} Lionel Porcar,[⊥] Yun Liu,^{#,¶} and Wei-Ren Chen^{*,†}

[†]Neutron Scattering Division, Oak Ridge National Laboratory, Oak Ridge, Tennessee 37831, United States

[‡]Center for Nanophase Materials Sciences, Oak Ridge National Laboratory, Oak Ridge, Tennessee 37831, United States

[§]Materials Science and Technology Division, Oak Ridge National Laboratory, Oak Ridge, Tennessee 37831, United States

^{||}Department of Materials Science and Engineering and Department of Physics and Astronomy, University of Tennessee, Knoxville, Tennessee 37996, United States

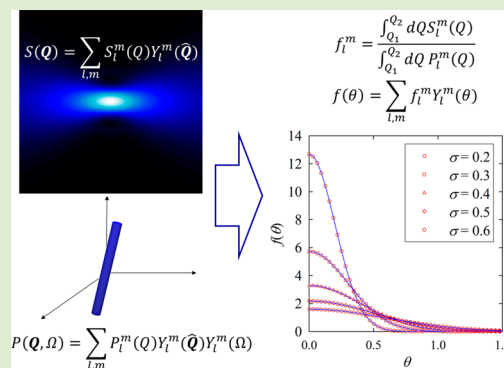
[⊥]Institut Laue-Langevin, B.P. 156, F-38042 Cedex 9 Grenoble, France

[#]The NIST Center for Neutron Research, National Institute of Standards and Technology, Gaithersburg, Maryland 20899-6100, United States

[¶]Department of Chemical Engineering, University of Delaware, Newark, Delaware 19716, United States

Supporting Information

ABSTRACT: We present a strategy for quantitatively evaluating the field-induced alignment of nonspherical particles using small-angle scattering techniques. The orientational distribution function (ODF) is determined from the anisotropic scattering intensity via the scheme of real spherical harmonic expansion. Our developed approach is simple and analytical and does not require a presumptive hypothesis of the ODF as an input in data analysis. A model study of aligned rigid rods demonstrates the validity of this proposed approach to facilitate the quantitative structural characterization of materials with preferred orientational states.



Elongated particles with an electric or magnetic dipole align under an applied electric or magnetic field. Understanding how the external fields affect the orientational ordering has great relevance to both applied as well as fundamental research endeavors. For example, with the presence of an electric field, the constituting molecules of liquid crystals change their orientation to align the axis of electric susceptibility with the direction of the applied field.^{1,2} The angular distribution of molecular orientation has been recognized to be essential to the electrical and optical properties of liquid-crystal-based devices.³ Moreover, in exploring the phase behavior in colloidal rods, the orientational distribution has been identified as the order parameter in the theoretical description of transition from a disorder to a liquid crystalline state.^{4–7}

There has been much interest in probing the orientational distribution function (ODF) of aligned particles experimentally.^{3,8–12} Among the available tools, small-angle scattering techniques provide the spatial resolution at the length scale relevant to the orientating structural units.^{13–24} The general experimental procedure, exemplified by a three-dimensional assembly of rigid rods, is given in Figure 1. The scheme is defined by the directions of incident beam (\hat{y}) and applied field

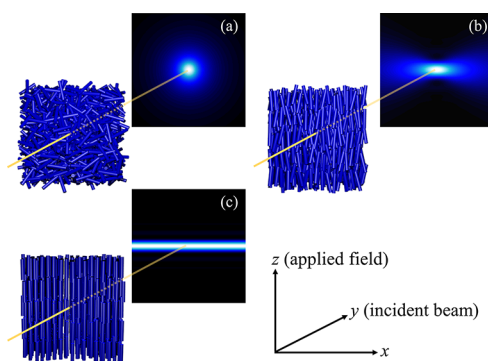


Figure 1. Schematic representations of using small-angle scattering techniques to investigate the orientation of rigid rods in (a) isotropic, (b) nematic, and (c) crystalline phases.

Received: June 28, 2019

Accepted: August 22, 2019

Published: September 17, 2019

(\hat{z}). The scattering intensity is therefore collected in the xz plane. For randomly oriented rods (Figure 1a), one normally sees a circularly isotropic intensity on the two-dimensional detector which faces perpendicularly to the incident beam because the scattering signal is orientationally averaged. Upon increasing the strength of the applied field, the isotropic scattering intensity on the detector plane becomes anisotropic progressively due to the alignment of rods. As demonstrated in Figure 1b, a stronger correlation would appear in the Q_x direction and a weaker correlation peak in the Q_z direction. If the rods are exactly parallel to one another to form a crystalline phase as shown in Figure 1c, the angular dependence of scattering data caused by the orientationally averaged systems is completely removed, and the spectrum is seen to keep its intensity practically constant along the Q_x direction. Nevertheless, for colloidal rods immersed in solutions, this perfect arrangement rarely occurs because of the configurational fluctuation and local density inhomogeneity caused by the Brownian motion.

The focus of this study is placed on extracting the orientational parameters of partially aligned particles from their anisotropic spectra such as the one given in Figure 1b. In a nematic system, the scattered intensity from the interparticle spatial correlation approaches unity in the high Q limit because of the lack of translational periodicity. Within this regime, the collected scattered intensity is essentially only contributed by the intraparticle correlation. As a result, the high Q part of the coherent scattering intensity is of particular relevance because the anisotropic scattering intensity is a direct manifestation of the ODF of constituting particles.^{14,25} A brief review about the existing methods for determining ODF from scattering measurements is helpful to demonstrate the motivation of our study: One popular approach to obtain the orientational parameters is through model fitting of small-angle scattering data based on a predetermined ODF.^{14,20,21,25–28} The validity of a selected ODF nevertheless is not known *a priori*. Alternatively, several model-free approaches have also been developed to determine the orientational order from the anisotropic diffraction patterns with varying degrees of success.^{29–33} The analyses have only been carried out over a limited Q range where the Bragg peak is observed. However, as evidenced by Figure 1b, for small-angle scattering data the information on orientational ordering is concealed in the characteristic spectral anisotropy manifesting over a wide range of Q . How to implement this existing scheme to small-angle scattering studies in a mathematically tractable manner is questionable.

Before proceeding, a comment should be made in regard to the evolution of the radius of gyration R_g of a particle when it undergoes a rotational motion. Earlier we showed that R_g^2 is the source term of intraparticle structure factor $S(\mathbf{Q})$ at the mean-field limit,³⁴ namely

$$R_g^2 = -\frac{1}{2} \nabla_{\mathbf{Q}}^2 S(\mathbf{Q})|_{\mathbf{Q}=0} \quad (1)$$

where $\nabla_{\mathbf{Q}}^2$ is the Laplacian operator in a reciprocal space. For a particle that does not deform or change its shape, its $S(\mathbf{Q})$ can be expressed as

$$S(\mathbf{Q}) = \int d\Omega P(\mathbf{Q}, \Omega) f(\Omega) \quad (2)$$

where Ω is the solid angle, $P(\mathbf{Q}, \Omega)$ the intraparticle structure factor at the specific orientation of Ω , and $f(\Omega)$ the ODF. Substituting eq 2 into eq 1, one finds that

$$R_g^2 = -\frac{1}{2} \nabla^2 P(\mathbf{Q}, \Omega)|_{\mathbf{Q}=0} \quad (3)$$

Equation 3 can be further extended to address the effect of polydispersity

$$R_g^2 = -\frac{1}{2} \langle \nabla^2 P(\mathbf{Q}, \Omega)|_{\mathbf{Q}=0} \rangle \quad (4)$$

where $\langle \rangle$ is the average over the size distribution. Based on the geometric nature of Laplacian, eqs 3 and 4 suggest that only dimensional and shape changes cause the variation of $S(\mathbf{Q})$. Therefore, for a rigid particle undergoing a rotational motion, its R_g remains invariant as required by its definition. This statement is validated by the results of theoretical calculation given in Figure 2: The change in the axial orientation of a rigid

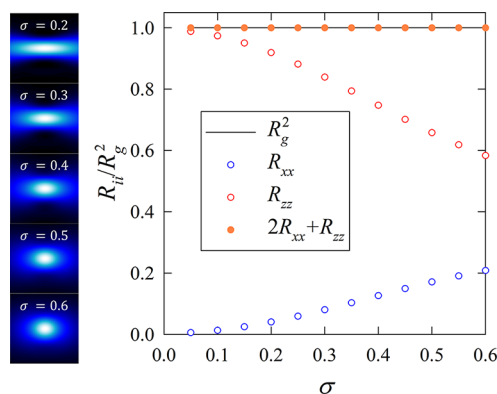


Figure 2. Theoretical calculation to explore how R_g^2 of a rigid rod evolves upon changing its axial orientation. The left panel gives the evolution of scattering spectra which are predicted by a Gaussian model of ODF given in eq 11. σ is the variance of the ODF. It is noted that randomly oriented rods are represented by the case of $\sigma = \infty$. The definition of the principal directions of scattering is identical to those in Figure 1. The right panel gives the evolution of the diagonal components of the gyration tensor as a function of σ . The black solid line defines the value of R_g^2 for a rigid rod. Within the probed range of σ , $2R_{xx} + R_{zz}$, the summation of the diagonal components of the gyration tensor is seen to be identical to R_g^2 .

rod is seen to result in a steady development in the spectral anisotropy. However, $2R_{xx} + R_{zz}$, the summation of the diagonal components of the gyration tensor, is seen to be identical to R_g^2 .

In this study, we use the real spherical harmonic expansion (RSHE) as the mathematical framework to analyze the anisotropic scattering spectra. It is instructive to briefly review the historical development of its application for the analysis of anisotropic structure. First suggested by Pryde,³⁵ extensive computational effort has been devoted to investigating the flow-induced structural distortion of simple liquids from the spherical harmonic expansion analysis of three-dimensional trajectories.^{36–38} There has also been much interest in examining the structure of flowing colloids from the scattering experiments using the same scheme.^{39–41} However, the loss of orthonormality of spherical harmonics basis vectors in the two-dimensional scattering intensities, which severely compounds the three-dimensional structural reconstruction, was not properly addressed until recently.^{42,43} Based on this approach,

for a rigid rod having a certain angle of the rod axis with respect to the alignment axis, one can express the corresponding $S(\mathbf{Q})$ as a linear combination of real spherical harmonics (RSH), namely

$$S(\mathbf{Q}) = \sum_{l,m} S_l^m(Q) Y_l^m(\hat{\mathbf{Q}}) \quad (5)$$

where l runs from $-\infty$ to ∞ and m from $-l$ to l ; $Q \equiv |\mathbf{Q}|$, $\hat{\mathbf{Q}}$ is the unit vector in \mathbf{Q} direction; and Y_l^m is the RSH of order l and degree m . Based on eq 5, one can express the generalized Guinier law as

$$S_0^0(Q) = 1 - \frac{Q^2}{3} R_g^2 + O(Q^4) \quad (6)$$

where $S_0^0(Q)$ is the isotropic component of $S(\mathbf{Q})$. Equations 3 and 6 serve as a sufficient condition for orientating rigid particles: The corresponding $S_0^0(Q)$ must remain invariant in the Guinier regime, regardless of their orientations. It also demonstrates that the anisotropic components $S_l^m(Q)$ in eq 5 are the results of the orientational correlation.

This calculation provides an initial clue suggesting that $f(\Omega)$ can be extracted from the analysis of $S(\mathbf{Q})$. The first step in this analysis approach is to provide the mathematical expressions of $P(\mathbf{Q}, \Omega)$ and $f(\Omega)$. Because of the completeness of RSH, one can, respectively, expand $P(\mathbf{Q}, \Omega)$ and $f(\Omega)$ as

$$P(\mathbf{Q}, \Omega) = \sum_{l,m} P_l^m(Q) Y_l^m(\hat{\mathbf{Q}}) Y_l^m(\Omega) \quad (7)$$

and

$$f(\Omega) = \sum_{l,m} f_l^m Y_l^m(\Omega) \quad (8)$$

where $P_l^m(Q)$ and f_l^m are coefficients associated with the basis vector of $Y_l^m(\Omega)$. From eq 2 and the orthonormality of RSH, it is found

$$f_l^m = \frac{\int_{Q_1}^{Q_2} dQ S_l^m(Q)}{\int_{Q_1}^{Q_2} dQ P_l^m(Q)} \quad (9)$$

From eqs 5 and 7, it is found that

$$S_l^m(Q) = \frac{1}{4\pi} \int d\hat{\mathbf{Q}} S(\mathbf{Q}) Y_l^m(\hat{\mathbf{Q}}) \quad (10)$$

and

$$P_l^m(Q) = \frac{1}{16\pi^2} \int d\hat{\mathbf{Q}} d\Omega P(\mathbf{Q}, \Omega) Y_l^m(\hat{\mathbf{Q}}) Y_l^m(\Omega) \quad (11)$$

$[Q_1, Q_2]$ in eq 9 gives the Q range which is relevant to the intraparticle spatial correlation. It is important to point out that $P(\mathbf{Q}, \Omega)$ can be determined either from a selected model of scattering function with a known mathematical expression or via the model-free inversion numerical procedures.⁴⁴ Because f_l^m can be expressed as a function of $S_l^m(Q)$ and $P_l^m(Q)$, via the scheme of RSH, the spectrum decomposition of both $P(\mathbf{Q}, \Omega)$ and $S(\mathbf{Q})$ allows the determination of $f(\Omega)$.

To verify the validity of this approach, we conduct a benchmarking study of an assembly of rigid rods with different degrees of alignment. The length and the diameter of a rigid rod are, respectively, l and d . The $P(\mathbf{Q}, \Omega)$ of an oriented rigid rod takes the analytic form

$$P(\mathbf{Q}, \Omega) = \left[2j_0\left(\frac{Ql}{2} \cos \gamma\right) \frac{J_1(Qd \sin \gamma)}{Qd \sin \gamma} \right]^2 \quad (12)$$

where γ is the angle between \mathbf{Q} and the rod axis, $j_0(x)$ the spherical Bessel function of order 0, and $J_1(x)$ the first-order Bessel function of the first kind. The relevant coefficients $P_l^m(Ql/2)$ extracted based on the RSH expansion given in eq 7 are given in Figures 3a and 3b.

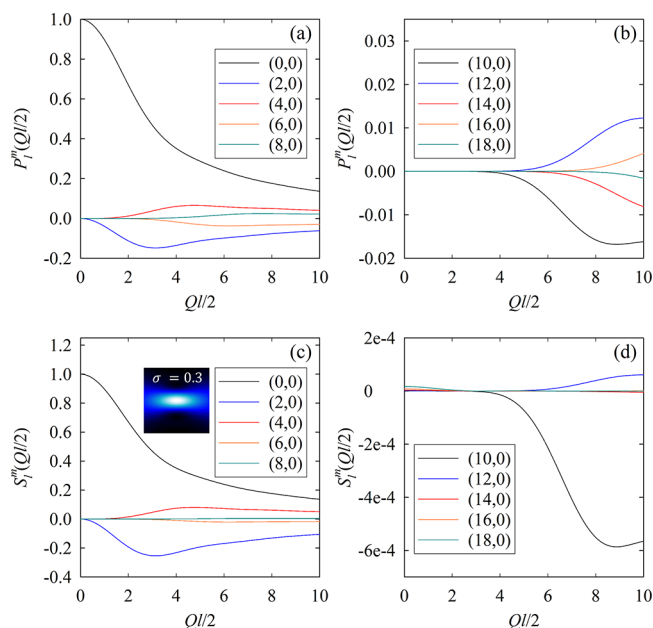


Figure 3. (a) and (b): Relevant coefficients of $P(\mathbf{Q}, \Omega)$ determined from eqs 7 and 12. The results are presented in a dimensionless unit of $Ql/2$ where l is the length of the rigid rod. (c) and (d): The coefficients of $S(\mathbf{Q})$ obtained from the RSH expansion of the spectrum given in the inset. The spectrum is predicted for an assembly of rigid rods characterized by an ODF given in eq 13 with $\sigma = 0.3$. The length-to-diameter ratio of a single rod is 15.

To simplify the calculation, we further assume the applied field is uniform along the z direction. Accordingly, $f(\Omega)$ is independent of the azimuthal angle ϕ in the xy plane and only a function of the polar angle θ with respect to z direction. As a result, $f(\Omega)$ can be expressed as $f(\theta)/2\pi$. Because of this cylindrical rotational symmetry, both $f(\theta)$ and $S(\mathbf{Q})$ are isotropic in the xy plane and must be a linear combination of basis vectors $Y_l^0(\theta)$, which form a complete set on xz and yz planes. Because of this property, $f(\Omega)$ can be reconstructed via eq 9 on both xz and yz planes. There exist several mathematical expressions of $f(\theta)$ developed for various materials.^{26,45–47} The following Gaussian functions are used as the ODF in our model study

$$f(\theta) = \begin{cases} A \exp\left(-\frac{\theta^2}{2\sigma^2}\right), & 0 \leq \theta < \frac{\pi}{2} \\ A \exp\left[-\frac{(\theta - \pi)^2}{2\sigma^2}\right], & \frac{\pi}{2} \leq \theta \leq \pi \end{cases} \quad (13)$$

where A is the normalization constants to ensure $\int_0^\pi f(\theta) \sin \theta d\theta = 1$. σ is the variance of $f(\theta)$. It is instructive to point out that the angular distribution in θ must be symmetrical with respect to $\theta = \pi/2$ due to the requirement of the cylindrical

symmetry of a rigid rod. An example of decomposed $S_l^m(Q)$ for an assembly of aligned rods with $\sigma = 0.3$ is given in Figures 3c and 3d. More examples are given in the Supporting Information.

Figure 4 presents the comparison between the $f(\theta)$ determined from the spectral analysis based on the proposed

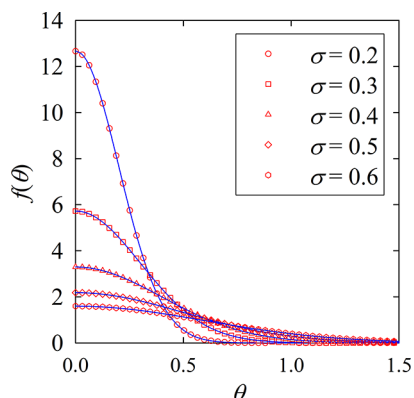


Figure 4. Comparisons between the orientational distribution functions determined from the spectral analysis based on eq 9 (red symbols) and exact theoretical $f(\theta)$ (blue curves) in eq 13.

RSH decomposition approach and the exact theoretical $f(\theta)$ used to generate the scattering spectra. The excellent agreements verify the usefulness of this approach in facilitating the related quantitative scattering studies of field-induced structural anisotropy in materials.

In summary, we have developed an approach to quantitatively evaluate the orientational ordering of field-aligned particles from their small-angle scattering intensities. Based on the expansion of real spherical harmonics, it is demonstrated that the orientational distribution functions can be determined experimentally by analyzing the spectral anisotropy. Our approach is applied to analyze the scattering spectra of an assembly of rigid rods with different degrees of axial alignment, and its validity of extracting ODF is theoretically verified. In comparison to the existing approaches to determine ODF from small-angle scattering measurements, our method does not require a predetermined mathematical expression of ODF as an input to obtain the orientational ordering and therefore provide a useful solution to bypass the potential issue of biased interpretation of experimental data. Another advantage is that our proposed approach can be applied to extract the ODF of aligned rigid particles with any geometric anisotropy.

Considerable efforts using scattering techniques have been devoted to investigating the shear-induced orientational ordering in soft materials such as flowing linear micelles and polymers.^{48–56} Our proposed approach can also be applied to facilitate the related studies. It can be foreseen that this extension might require us to address the issue of the lack of cylindrical symmetry. However, the mathematical treatment should remain tractable. Moreover, having established a rigorous approach for determining the ODF of rigid particles from their anisotropic scattering intensities, the question of determining the orientational parameters and related structural information on materials consisting of particles with flexible molecular conformations can now be addressed. By analyzing the anisotropic scattering spectra in the reciprocal space relevant to the single-particle conformation, the orientational

ordering of aligned particles can be extracted from their anisotropy of their scattering spectra based on the theoretical framework introduced in this work.⁵⁷ An experimental study of aligning rod-like micelles in Couette flow given in the Supporting Information indeed demonstrates the feasibility of our approach for facilitating the quantitative scattering investigation of this important field of soft matter study.

■ ASSOCIATED CONTENT

📄 Supporting Information

The Supporting Information is available free of charge on the ACS Publications website at DOI: 10.1021/acsmacrolett.9b00496.

$S_l^m(Q)$ for different σ ; tables of f_l^m for different σ ; and an example of probing the orientational ordering of rod-like micelles subjected to steady shear (PDF)

■ AUTHOR INFORMATION

Corresponding Authors

*E-mail: huangrn@ornl.gov.

*E-mail: chenw@ornl.gov.

ORCID

Yangyang Wang: 0000-0001-7042-9804

Yuya Shinohara: 0000-0001-8284-751X

Yun Liu: 0000-0002-0944-3153

Wei-Ren Chen: 0000-0002-5192-0777

Notes

The authors declare no competing financial interest.

■ ACKNOWLEDGMENTS

This research was supported by the Laboratory Directed Research and Development Program of Oak Ridge National Laboratory, managed by UT-Battelle, LLC, for the U.S. Department of Energy, and performed at SNS and CNMS, which are DOE Office of Science User Facilities operated by the Oak Ridge National Laboratory. Y.S. and T.E. are supported by the U.S. Department of Energy, Office of Science, Office of Basic Energy Sciences, Materials and Science and Engineering Division. Access to NGB30mSANS was provided by the Center for High Resolution Neutron Scattering, a partnership between the National Institute of Standards and Technology and National Science Foundation under Agreement No. DMR-1508249. We gratefully appreciate the D22 SANS beamtime from ILL.

■ REFERENCES

- (1) de Gennes, P.-G. *The Physics of Liquid Crystals*; Oxford University Press Inc.: New York, 1993.
- (2) Collings, P. J. *Liquid Crystals: Nature's Delicate Phase of Matter*; Princeton University Press: Princeton, 2001.
- (3) Takato, K.; Hasegawa, M.; Koden, M.; Itoh, N.; Hasegawa, R.; Sakamoto, M. *Alignment Technologies and Applications of Liquid Crystals*; Taylor & Francis: London, 2005.
- (4) Lee, S.-D.; Meyer, R. B. Computations of the Phase Equilibrium, Elastic Constants, and Viscosities of a Hard-Rod Nematic Liquid Crystal. *J. Chem. Phys.* **1986**, *84*, 3443–3448.
- (5) Graf, H.; Löwen, H. Phase Diagram of Tobacco Mosaic Virus Solutions. *Phys. Rev. E: Stat. Phys., Plasmas, Fluids, Relat. Interdiscip. Top.* **1999**, *59*, 1932–1942.
- (6) Savenko, S. V.; Dijkstra, M. Sedimentation and Multiphase Equilibria in Suspensions of Colloidal Hard Rods. *Phys. Rev. E* **2004**, *70*, No. 051401.

- (7) Drwenski, T.; Dussi, S.; Hermes, M.; Dijkstra, M.; van Roij, R. Phase Diagrams of Charged Colloidal Rods: Can a Uniaxial Charge Distribution Break Chiral Symmetry? *J. Chem. Phys.* **2016**, *144*, No. 094901.
- (8) Picken, S. J. Orientational Order in Aramid Solutions Determined by Diamagnetic Susceptibility and Birefringence Measurements. *Macromolecules* **1990**, *23*, 464–470.
- (9) Pérez, R.; Banda, S.; Ounaies, Z. Determination of the Orientation Distribution Function in Aligned Single Wall Nanotube Polymer Nanocomposites by Polarized Raman Spectroscopy. *J. Appl. Phys.* **2008**, *103*, No. 074302.
- (10) Castelletto, V.; Newby, G. E.; Zhu, Z.; Hamley, I. W.; Noirez, L. Self-Assembly of PEGylated Peptide Conjugates Containing a Modified Amyloid β -Peptide Fragment. *Langmuir* **2010**, *26*, 9986–9996.
- (11) Taniguchi, S.; Koyama, D.; Shimizu, Y.; Emoto, A.; Nakamura, K.; Matsukawa, M. Control of Liquid Crystal Molecular Orientation Using Ultrasound Vibration. *Appl. Phys. Lett.* **2016**, *108*, 101103.
- (12) Tan, Y. Z.; Baldwin, P. R.; Davis, J. H.; Williamson, J. R.; Potter, C. S.; Carragher, B.; Lyumkis, D. Addressing Preferred Specimen Orientation in Single-Particle Cryo-EMEM through Tilting. *Nat. Methods* **2017**, *14* (8), 793–796.
- (13) Hayter, J. B.; Pynn, R.; Charles, S.; Skjeltorp, A. T.; Trehwella, J.; Stubbs, G.; Timmins, P. Ordered Macromolecular Structures in Ferrofluid Mixtures. *Phys. Rev. Lett.* **1989**, *62*, 1667–1670.
- (14) Groot, L. C. A.; Kuil, M. E.; Leyte, J. C.; van der Maarel, J. R. C.; Heenan, R. K.; King, S. M.; Jannink, G. Neutron Scattering Experiments on Magnetically Aligned Liquid Crystalline DNA Fragment Solutions. *Liq. Cryst.* **1994**, *17*, 263–276.
- (15) Davidson, P.; Bourgaux, C.; Sergot, P.; Livage, J. A Small-Angle X-ray Scattering Study of the Lyotropic Nematic Phase of Vanadium Pentoxide Gels. *J. Appl. Crystallogr.* **1997**, *30*, 727–732.
- (16) Picken, S. J.; Noirez, L.; Luckhurst, G. R. Molecular Conformation of a Polyaramid in Nematic Solution from Small Angle Neutron Scattering and Comparison with Theory. *J. Chem. Phys.* **1998**, *109*, 7612–7617.
- (17) Elliott, J. A.; Hanna, S.; Elliott, A. M. S.; Cooley, G. E. Interpretation of the Small-Angle X-ray Scattering from Swollen and Oriented Perfluorinated Ionomer Membranes. *Macromolecules* **2000**, *33*, 4161–4171.
- (18) Lemaire, B. J.; Davidson, P.; Panine, P.; Jolivet, J. P. Magnetic-Field-Induced Nematic-Columnar Phase Transition in Aqueous Suspensions of Goethite (α -FeOOH) Nanorods. *Phys. Rev. Lett.* **2004**, *93*, 267801.
- (19) Gilroy, J. B.; Gädt, T.; Whittell, G. R.; Chabanne, L.; Mitchels, J. M.; Richardson, R. M.; Winnik, M. A.; Manners, I. Monodisperse Cylindrical Micelles by Crystallization-Driven Living Self-Assembly. *Nat. Chem.* **2010**, *2*, 566–570.
- (20) Viamontes, J.; Narayanan, S.; Sandy, A. R.; Tang, J. X. Orientational Order Parameter of the Nematic Liquid Crystalline Phase of F-actin. *Phys. Rev. E* **2006**, *73*, No. 061901.
- (21) Hamley, I. W.; Krysmann, M. J.; Newby, G. E.; Castelletto, V.; Noirez, L. Orientational Ordering in the Nematic Phase of a Polyethylene Glycol–Peptide Conjugate in Aqueous Solution. *Phys. Rev. E* **2008**, *77*, No. 062901.
- (22) Märkert, C.; Fischer, B.; Wagner, J. Small-Angle Scattering from Spindle-Shaped Colloidal Hematite Particles in External Magnetic Fields. *J. Appl. Crystallogr.* **2011**, *44*, 441–447.
- (23) Gilroy, J. B.; Rugar, P. A.; Whittell, G. R.; Chabanne, L.; Terrill, N. J.; Winnik, M. A.; Manners, I.; Richardson, R. M. Probing the Structure of the Crystalline Core of Field-Aligned, Monodisperse, Cylindrical Polyisoprene-*block*-Polyferrocenylsilane Micelles in Solution Using Synchrotron Small- and Wide-Angle X-ray Scattering. *J. Am. Chem. Soc.* **2011**, *133*, 17056–17062.
- (24) Hayward, D. W.; Gilroy, J. B.; Rugar, P. A.; Chabanne, L.; Pizzey, C.; Winnik, M. A.; Whittell, G. R.; Manners, I.; Richardson, R. M. Liquid Crystalline Phase Behavior of Well-Defined Cylindrical Block Copolymer Micelles Using Synchrotron Small-Angle X-ray Scattering. *Macromolecules* **2015**, *48*, 1579–1591.
- (25) Purdy, K. R.; Dogic, Z.; Fraden, S.; Rühm, A.; Lurio, L.; Mochrie, S. G. J. Measuring the Nematic Order of Suspensions of Colloidal fd Virus by X-ray Diffraction and Optical Birefringence. *Phys. Rev. E: Stat. Phys., Plasmas, Fluids, Relat. Interdiscip. Top.* **2003**, *67*, No. 031708.
- (26) Oldenbourg, R.; Wen, X.; Meyer, R. B.; Caspar, D. L. D. Orientational Distribution Function in Nematic Tobacco-Mosaic-Virus Liquid Crystals Measured by X-Ray Diffraction. *Phys. Rev. Lett.* **1988**, *61*, 1851–1854.
- (27) Hamley, I. W.; Castelletto, V.; Moulton, C.; Myatt, D.; Siligardi, G.; Oliveira, C. L. P.; Pedersen, J. S.; Abutbul, I.; Danino, D. Self-Assembly of a Modified Amyloid Peptide Fragment: pH-Responsiveness and Nematic Phase Formation. *Macromol. Biosci.* **2010**, *10*, 40–48.
- (28) Zhang, F.; Heiney, P. A.; Srinivasan, A.; Naciri, J.; Ratna, B. Structure of Nematic Liquid Crystalline Elastomers under Uniaxial Deformation. *Phys. Rev. E* **2006**, *73*, No. 021701.
- (29) Leadbetter, A. J.; Norris, E. K. Distribution Functions in Three Liquid Crystals from X-Ray Diffraction Measurements. *Mol. Phys.* **1979**, *38*, 669–686.
- (30) Davidson, P.; Petermann, D.; Levelut, A. The Measurement of the Nematic Order Parameter by X-Ray Scattering Reconsidered. *J. Phys. II* **1995**, *5*, 113–131.
- (31) Deutsch, M. Orientational Order Determination in Liquid Crystals by X-Ray Diffraction. *Phys. Rev. A: At., Mol., Opt. Phys.* **1991**, *44*, 8264–8270.
- (32) Lovell, R.; Mitchell, G. R. Molecular Orientation Distribution Derived from an Arbitrary Reflection. *Acta Crystallogr., Sect. A: Cryst. Phys., Diff., Theor. Gen. Crystallogr.* **1981**, *A37*, 135–137.
- (33) Mitchell, G. R.; Windle, A. H. Orientation in Liquid Crystal Polymers. In *Developments in Crystalline Polymers-2*; Bassett, D. C., Eds.; Elsevier Applied Science: London and New York, 1988.
- (34) Huang, G.-R.; Wang, Y.; Do, C.; Porcar, L.; Shinohara, Y.; Egami, T.; Chen, W. R. Determining Gyration Tensor of Orienting Macromolecules through Their Scattering Signature. *J. Phys. Chem. Lett.* **2019**, *10*, 3978–3984.
- (35) Pryde, J. A. *The Liquid State*; Hutchison University Library: London, 1966.
- (36) For example, see: Ashurst, W. T.; Hoover, W. G. Dense-Fluid Shear Viscosity via Nonequilibrium Molecular Dynamics. *Phys. Rev. A: At., Mol., Opt. Phys.* **1975**, *11*, 658–678.
- (37) Evans, D. J.; Hanley, H. J. M.; Hess, S. Non-Newtonian phenomena in Simple Fluids. *Phys. Today* **1984**, 27–33.
- (38) Evens, D. J.; Morriss, G. *Statistical Mechanics of Nonequilibrium Liquids*; Cambridge University Library: Cambridge, 2008.
- (39) Johnson, S. J.; de Kruif, C. G.; May, R. P. Structure Factor Distortion for Hard-Sphere Dispersions Subjected to Weak Shear Flow: Small-Angle Neutron Scattering in the Flow-Vorticity Plane. *J. Chem. Phys.* **1988**, *89*, 5909–5921.
- (40) Wagner, N. J.; Russel, W. B. Light Scattering Measurements of a Hard-Sphere Suspension under Shear. *Phys. Fluids A* **1990**, *2*, 491–502.
- (41) Wagner, N. J.; Ackerson, B. J. Analysis of Nonequilibrium Structures of Shearing Colloidal Suspensions. *J. Chem. Phys.* **1992**, *97*, 1473–1483.
- (42) Huang, G.-R.; Wang, Y.; Wu, B.; Wang, Z.; Do, C.; Smith, G. S.; Bras, W.; Porcar, L.; Falus, P.; Chen, W.-R. Reconstruction of Three-Dimensional Anisotropic Structure from Small-Angle Scattering Experiments. *Phys. Rev. E: Stat. Phys., Plasmas, Fluids, Relat. Interdiscip. Top.* **2017**, *96*, No. 022612.
- (43) Huang, G.-R.; Wang, Y.; Wu, B.; Chen, W.-R. Characterization of Microscopic Deformation through Two-Point Spatial Correlation Functions. *Phys. Rev. E: Stat. Phys., Plasmas, Fluids, Relat. Interdiscip. Top.* **2018**, *97*, No. 012605.
- (44) Lindner, P. In *Neutron, X-rays and Light. Scattering Methods Applied to Soft Condensed Matter*; Lindner, P., Zemb, Th., Eds.; North-Holland: Amsterdam, 2002.
- (45) Onsager, L. The Effects of Shape on the Interaction of Colloidal Particles. *Ann. N. Y. Acad. Sci.* **1949**, *51*, 627–659.

(46) Maier, W.; Saupe, A. Eine Einfache Molekulare Theorie des Nematichen Kristallinflüssigen Zustande. *Z. Naturforsch., A: Phys. Sci.* **1958**, *13A*, 564–566.

(47) Odijk, T. Theory of Lyotropic Polymer Liquid-Crystals. *Macromolecules* **1986**, *19*, 2313–2329.

(48) Hayter, J. B.; Penfold, J. Use of Viscous Shear Alignment to Study Anisotropic Micellar Structure by Small-Angle Neutron Scattering. *J. Phys. Chem.* **1984**, *88*, 4589–4593.

(49) Berret, J.-F.; Roux, D. C.; Porte, G.; Lindner, P. Tumbling Behaviour of Nematic Worm-like Micelles under Shear Flow. *Europhys. Lett.* **1995**, *32*, 137–142.

(50) Ugaz, V. M.; Burghardt, W. R. In Situ X-ray Scattering Study of a Model Thermotropic Copolyester under Shear: Evidence and Consequences of Flow-Aligning Behavior. *Macromolecules* **1998**, *31*, 8474–8484.

(51) Mendes, E.; Viale, S.; Santin, O.; Heinrich, M.; Picken, S. J. A Small-Angle Neutron Scattering Investigation of Rigid Polyelectrolytes under Shear. *J. Appl. Crystallogr.* **2003**, *36*, 1000–1005.

(52) Singh, M.; Agarwal, V.; Kee, D. D.; McPherson, G.; John, V.; Bose, A. Shear-Induced Orientation of a Rigid Surfactant Mesophase. *Langmuir* **2004**, *20*, 5693–5702.

(53) Förster, S.; Konrad, M.; Lindner, P. Shear Thinning and Orientational Ordering of Wormlike Micelles. *Phys. Rev. Lett.* **2005**, *94*, No. 017803.

(54) Nakamura, K.; Shikata, T. Small Angle Neutron Scattering Study of Polyelectrolyte Conformation Incorporated into Hybrid Threadlike Micelles under Strong Shear Flows. *J. Phys. Chem. B* **2007**, *111*, 12411–12417.

(55) Angelico, R.; Rossi, C. O.; Ambrosone, L.; Palazzo, G.; Mortensen, K.; Olsson, U. Ordering Fluctuations in a Shear-Banding Wormlike Micellar System. *Phys. Chem. Chem. Phys.* **2010**, *12*, 8856–8862.

(56) Hamley, I. W.; Burholt, S.; Hutchinson, J.; Castelletto, V.; da Silva, E. R.; Alves, W.; Gutfreund, P.; Porcar, L.; Dattani, R.; Hermida-Merino, D.; Newby, G.; Reza, M.; Ruokolainen, J.; Stasiak, J. Shear Alignment of Bola-Amphiphilic Arginine-Coated Peptide Nanotubes. *Biomacromolecules* **2017**, *18*, 141–149.

(57) The computer code of calculating ODF from the scattering spectra will be incorporated into the data analysis protocol of EQ-SANS at SNS. It is also available from WRC (e-mail: chenw@ornl.gov).